International Conference on Mechanical, Industrial and Materials Engineering 2015 (ICMIME2015)
11-13 December, 2015, RUET, Rajshahi, Bangladesh.

Paper ID: FM-09

Flow-Induced Vibration Mechanism of a Cylinder Immersed in a Wake

B. Qin[1], Md. Mahbub Alam[1, 2], Y. Zhou[1]
[1]Institute for Turbulence-Noise-Vibration Interaction and Control, Shenzhen Graduate School, Harbin Institute of Technology, Shenzhen, China
[2]Key Lab of Advanced Manufacturing Technology, School of Mechanical Engineering and Automation, Shenzhen Graduate School, Harbin Institute of Technology, Shenzhen, China
Email: alamm28@yahoo.com; alam@hitsz.edu.cn

Abstract

Flow-induced vibration response of a circular cylinder (diameter D) placed in the wake of a rigid circular cylinder of smaller diameter d is examined experimentally. The monitoring cylinder is both-end-spring-mounted, free to oscillate only in the cross-flow direction. D is kept fixed, d is varied from d/D = 0.2 to 1.0. The spacing L between the center of the upstream cylinder to the forward stagnation point of the downstream cylinder is changed from L/d = 1.0 to 5.5. Flow-induced vibration amplitude A/D, vortex shedding frequency, lift force and PIV measurements are conducted. A decreasing d/D causes a higher instability of flow, leading to violent vibration. Vortex shedding characteristics at some representative cases are elaborated. Two shear layers reattaching alternately on the downstream cylinder may excite the cylinder vibration. In addition, what happens during the start of vibration is explicated through measurements of added mass and added damping.

Keywords: Flow-induced vibration, Vortex shedding frequency, Different diameters, Lift force.

1. Introduction

The study of flow-induced vibrations (FIV) of a structure is important in many engineering fields, including aeronautical, offshore, power plant, civil, and wind engineering. Previous investigations have mostly been concerned with two rigid circular cylinders in tandem, paying attention to flow structures generated, forces acting on them, Strouhal frequencies, etc., [1]. Bokaian and Geoola [2] surveyed FIV of a both-end-spring-mounted cylinder immersed in the wake of a fixed identical upstream cylinder, where the downstream cylinder is free to oscillate laterally. The mass-damping ratio $m^*\zeta$ of the system is about 0.109 (where m^* = mass ratio, ζ = damping ratio). FIV characteristics of two circular cylinders in tandem have been investigated by Kim *et al.* [3], with L/d = 0.6 ~ 3.7, reduced velocity U_r = 1.5 ~ 26 and $m^*\zeta$ = 0.65. The FIV of a pair of cylinders in tandem has also been investigated by Assi *et al.* [4, 5] for $L/d \geq 4.0$ at $m^*\zeta$ = 0.013, where the mechanism of the origin of the downstream cylinder lift forces has been elucidated. Divergent vibration was observed for L/d = 4.0 ~ 6.0 with increasing U_r, and constant vibration amplitude was for L/d > 6.0. A review of previous researches connected with FIV of two tandem cylinders indicates that former investigations have mostly been with two identical diameter cylinders at a low $m^*\zeta$ value. A systematic study on the influence of the upstream cylinder size (diameter) on FIV of a downstream cylinder is very scarce. The objective of this work is to study experimentally FIV characteristics of a cylinder in the presence of an upstream fixed cylinder of which the diameter is changed.

2. Experiment details

FIV experiments were carried out in a low-speed, close-circuit wind tunnel with a test section of 5 m long, 0.8 m width and 1.0 m height. A schematic diagram of the experimental setup is shown in Fig. 1. The upstream cylinder diameter d was 8, 16, 24, 32 and 40 mm and the downstream cylinder diameter D was 40 mm, corresponding to d/D = 0.2, 0.4, 0.6, 0.8 and 1.0, respectively. L/d = 1.0, 1.5, 2.0, 2.5, 3.0, 3.5, 4.0 and 5.5 were chosen. The upstream cylinder was fixed at both ends. Each end of the downstream cylinder was supported by two spiral springs (Fig. 1c). A standard laser vibrometer was used to measure the vibration-amplitude (A) and vibration frequency of the downstream cylinder. ζ, $m^*\zeta$, and natural frequency of the cylinder (f_n) were estimated to be 0.0021, 0.58, and 11.72 Hz, respectively. Free-stream velocity U_∞ was varied from 1.8 to 10.3 m/s, corresponding to variation of U_r from 3.8 to 22.0 and of Re (based on D and U_∞) from 4.8×10^3 to 2.7×10^4. Two hot wires, one (HT1) placed in the gap at (x'/d, y'/d, z'/d) = (1, 1, 0), another (HT2) behind the downstream

cylinder at (*x/D, y/D, z/D*) = (4, 1, 0), were used to measure natural vortex shedding frequencies. Flow-induced forces and flow structures were measured by using a pressure scanner and a PIV system, respectively.

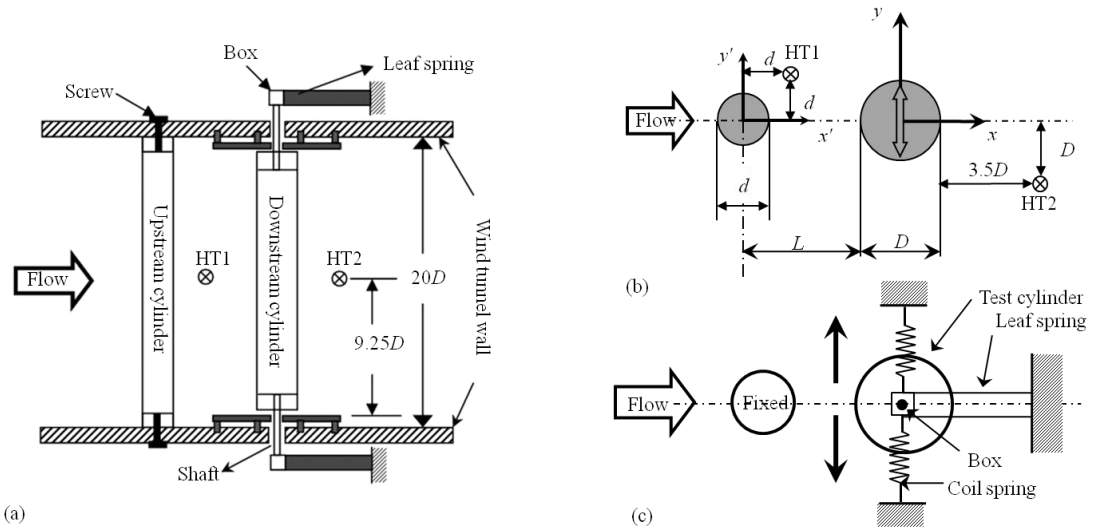

Fig. 1. Experimental setup (a) Experimental arrangement, (b) definition of symbols, (c) the test cylinder mounting system

3. Results and discussions

3.1. Vibration response

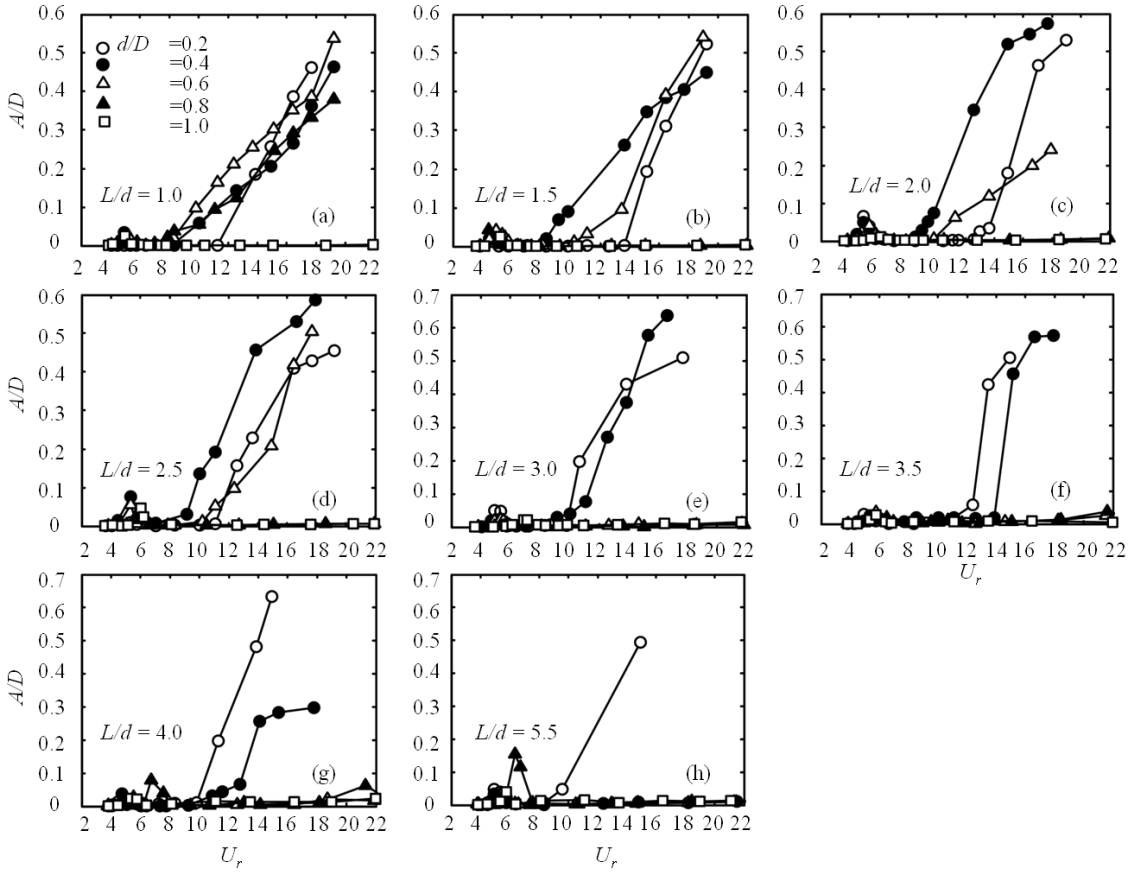

Fig. 2. FIV responses for different *d/D* at (a) *L/d* = 1.0, (b) *L/d* = 1.5, (c) *L/d* = 2.0, (d) *L/d* = 2.5, (e) *L/d* = 3.0, (f) *L/d* = 3.5, (g) *L/d* = 4.0, and (h) *L/d* = 5.5.

Fig. 2 presents the dependence of the cylinder vibration amplitude ratio (*A/D*) on *d/D* and *L/d*. At *L/d* = 1.0, violent and divergent vibrations occur for *d/D* = 0.2, 0.4, 0.6, 0.8 at U_r > 11.5, 8.8 and 8 respectively. Tiny humps engendered around U_r = 5 signify the occurrence of vortex-excitation (VE) (Fig. 2a). At 1.5 ≤ *L/d* ≤ 2.5 (Fig. 2b, c, d), *d/D* = 0.2, 0.4 and 0.6 generate vibrations, while *d/D* = 0.8 and 1.0 do not. As *L/d* is increased to 3.0 ~ 4.0 (Figs. 2e, f, g), vibration only appears for *d/D* = 0.2 and 0.4. Extending *L/d* further to 5.5 leads to vibration for *d/D* = 0.2 only (Fig. 2h). Thus, it can be inferred that a cylinder immersed in the wake of another of different diameter may undergo a catastrophic vibration, and a decrease in *d/D* results in a higher instability of flow.

3.2. Power spectral analysis results

Representative power spectral analysis results of HT2 and laser vibrometer signals at *d/D* = 0.4, *L/d* = 2.0 are presented in Fig. 3(a, b). f/f_n of the horizontal axis is the normalized Fourier frequency *f*. The peaks in the power spectra are extracted as f_v/f_n and plotted in Fig. 3(c). The corresponding vibration response is presented in Fig. 3(d) in order to have a mutual vibrant discussion between shedding frequency and vibration response. f_v/f_n = 1.0 at U_r = 4.5 ~ 5.3 is observed in both HT2 and laser vibrometer results (Fig. 3a, b). Convergent vibration occurs in this range of U_r (Fig. 3d), indicating VE, resonance and lock-in. As U_r goes beyond the lock-in range, $f_v/f_n \neq 1.0$, rising monotonically following *St* = 0.2 until U_r = 8.5. No vibration thus occurs at 5.3 < U_r < 8.5. With an increase in U_r, the cylinder begins to vibrate at U_r = 8.5 ~ 9.8, the vibration amplitude taking off; the second peak corresponding to f_v is more discernible (Fig. 3b) and HT2 results do not display peak at f_v/f_n = 1.0. The information indicates that the vibration is initiated by the vortex shedding from the cylinder, not by any shedding associated with f_n. On the other hand, when the amplitude is large enough (U_r > 9.8), there are two dominant peaks in the HT2 results (Fig. 3a), corresponding to vibration frequency (f_v/f_n = 1.0) and natural vortex shedding frequency as presented in Fig. 3(c). The latter frequency follows Strouhal number *St* = 0.2 up to U_r = 14.9 and then locks-in to the third harmonic of f_n for U_r > 14.9 where *A/D* escalation is restricted.

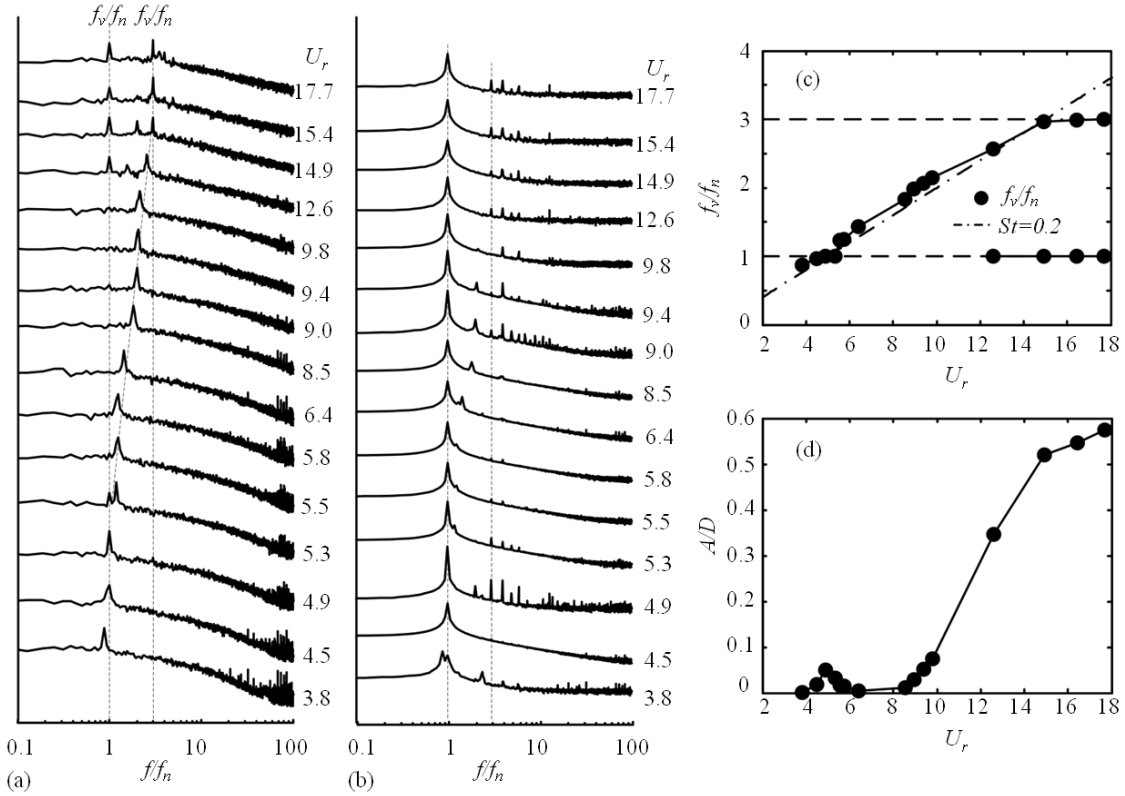

Fig. 3. Representative power spectral analysis results (a) Power spectrum of HT2 signal, (b) power spectrum of laser vibrometer signal, (c) vortex shedding frequency obtained from HT2, and (d) *A/D* variation with U_r. *d/D* = 0.4, *L/d* = 2.0.

3.3. Vibration mechanism

Fig. 4(a) shows the schematic plot of the cylinder displacement *y/D* and lift force coefficient C_L in a half cycle of oscillation at *L/d* = 2.0, *d/D* = 0.4, accompanied with the phase-average vorticity and pressure coefficient C_P (positive when the arrow points to the cylinder center) distributions (Fig. 4b ~ f). First, it is necessary to clarify that due to the additional cables mounted around the cylinder for measuring pressure, the *m**

and ζ have changed to 350 and 0.043, respectively. As the downstream cylinder moves upward, the upstream cylinder shear layer emanating from lower side reattaches on the lower side of the downstream cylinder at $\theta \approx -22.5°$ where $C_P \approx +1$ (Fig. 4b). A slice of the reattached flow together with the upper shear layer sweeping over the upper side of the downstream cylinder gives rise to a highly negative pressure on the upper side, resulting in an upward lift force. With the cylinder moving upward, the shear layer from upper side reattaches, resulting in the decay of lift. A maximum negative lift occurs as the upper shear layer passes over the lower side and stagnation pressure on the upper side is generated by the freestream flow (Fig. 4d, e). The cylinder thus speeds up downward.

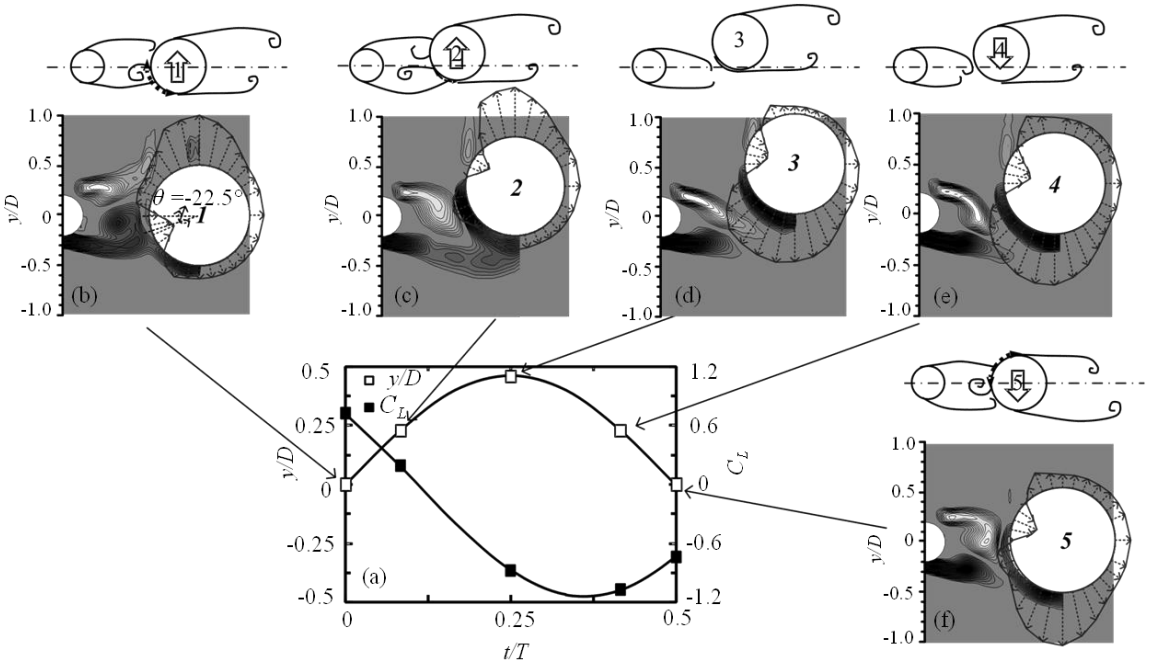

Fig. 4. (a) Cylinder displacement y/D and lift force coefficient C_L in half cycle of the oscillation, (b-f) phase-averaged vorticity and pressure coefficient C_P at L/d = 2.0, d/D = 0.4, A/D = 0.48.

3.4. Added mass coefficient and added damping ratio

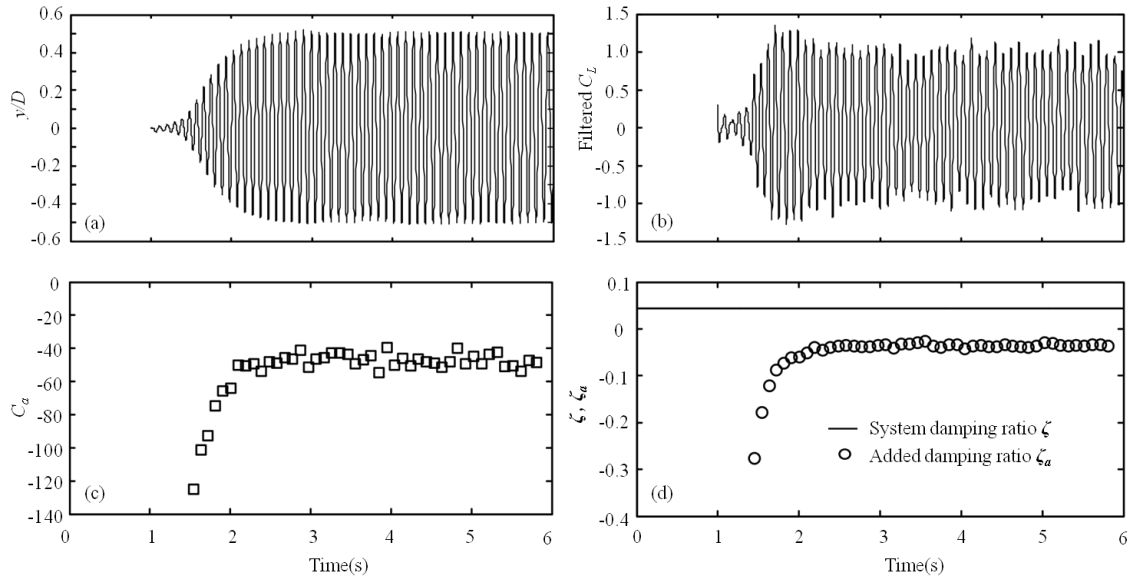

Fig. 5. Time history of (a): y/D, (b) filtered C_L, (c) added mass coefficient C_a, and (d) added damping ratio ζ_a when the downstream cylinder is fixed and then released at t = 1 s.

Fig. 5 (a, b) show the evolution of y/D and filtered C_L where the lift force is band-pass filtered by 5 ~ 20 Hz to contain only frequency component of the lift around the vibration frequency since others will not yield a net contribution to the energy transfer between the fluid and the body [6]. Note that the cylinder was kept fixed and

suddenly released at t = 1 s. At the same time, the maximum y/D (amplitude) in each cycle increases from ≈0 to 0.48 at t = 1 ~ 2.9 s, and then remains nearly constant (Fig. 5a). At t = 1 ~ 1.4 s where the cylinder starts to vibrate, C_L varies irregularly, being not sinusoidal. C_L then undergoes an increase in amplitude in each cycle reaching maximum at about t = 1.7 s, after which it suffers a small decrease before being approximately stable (Fig. 5b). Besides, the added mass coefficient C_a and added damping ratio ζ_a which are concerned with the lift force components in phase with the cylinder acceleration and velocity, respectively, are presented in Fig. 5 (c, d).

At t < 1.4 s, since the filtered C_L is not sinusoidal and the harmonic forcing and harmonic motion assumption is not applicable, the calculation of C_a and ζ_a starts at t = 1.4 s. The calculation method of C_a and ζ_a in each cycle can be found in [7]. C_a is highly negative -125 at $t \approx$ 1.4 s where the vibration starts, increasing to its asymptotic value -47 at $t \approx$ 2.3 s where the vibration is stable (Fig. 5c). $C_a \approx$ -47 at t > 2.3 s is much smaller than m^* = 350; cylinder vibration frequency hence does not differ from f_n. On the other hand, t < 2.3 s the vibration frequency increases upto 1.12f_n (not shown). Between t = 1.4 s and 2.3 s, ζ_a being negative escalates from -0.27 to -0.043; the magnitude of the latter is equal to the system damping ratio ζ (Fig. 5d). Thus it may be inferred that during the increase of the vibration amplitude, the cylinder sustains a negative effective damping ratio ($\zeta + \zeta_a < 0$), leading to an exponential growth of oscillation amplitude. On the contrary, at the stable vibration, nearly zero damping ratio is obtained ($\zeta + \zeta_a \approx 0$), which means that a balance is reached between the energy transferred from the fluid to the structure and the energy consumed by the system damping.

4. Conclusions

A violent vibration of the cylinder is observed for d/D = 0.2 ~ 0.8 at L/d = 1.0, for d/D = 0.2 ~ 0.6 at 1.0 < $L/d \leq$ 2.5, for d/D = 0.2 ~ 0.4 at 2.5 < $L/d \leq$ 4.0, and for d/D = 0.2 at 4.0 < $L/d \leq$ 5.5, but not for d/D = 1.0. A decreasing d/D is inclined to engender vibration for a longer range of L/d. For certain d/D - L/d cases, a lock-in of vortex shedding to the third harmonics of the cylinder vibration frequency is observed. Two shear layers of the upstream cylinder reattaching alternately on the downstream cylinder give rise to a large change in lift that maintains the vibration. A negative effective damping ratio ($\zeta + \zeta_a < 0$) leads to a growth in vibration amplitude where the energy transferred from the fluid to the structure is larger than the energy consumed by the system damping. On the other hand, at stable vibration condition, $\zeta + \zeta_a \approx 0$ is obtained, representing a balance between energy transfer and consumption.

Acknowledgments Alam wishes to acknowledge support given to him from the Research Grant Council of Shenzhen Government through grant KQCX2014052114423867, JCYJ20130402100505796 and JCYJ20120613145300404.

References

[1] M.M. Alam, M. Moriya, K. Takai, and H. Sakamoto, "Fluctuating fluid forces acting on two circular cylinders in a tandem arrangement at a subcritical Reynolds number", *Journal of Wind Engineering and Industrial Aerodynamics*, Vol.91, No.1, pp. 139-154, 2003.

[2] A. Bokaian, and F. Geoola, "Wake-induced galloping of two interfering circular cylinders", *Journal of Fluid Mechanics*, Vol.146, pp. 383-415, 1984.

[3] S. Kim, M.M. Alam, Sakamoto. H, and Zhou. Y, "Flow-induced vibrations of two circular cylinders in tandem arrangement, part 1: characteristics of vibration", *Journal of Wind Engineering and Industrial Aerodynamics*, Vol.97, No.5, pp. 304-311, 2009.

[4] G.R.S. Assi, P.W. Bearman, J.R. Meneghini, "On the wake-induced vibration of tandem circular cylinders: the vortex interaction excitation mechanism", *Journal of Fluid Mechanics*, Vol.661, pp. 365-401, 2010.

[5] G.R.S. Assi, P.W. Bearman, B.S. Carmo, J.R. Meneghini, S.J. Sherwin, and H.J. Willden, "The role of wake stiffness on the wake-induced vibration of the downstream cylinder of a tandem pair", *Journal of Fluid Mechanics*, Vol.718, pp. 210-245, 2013.

[6] T.L. Morse, and C.H.K. Williamson, "Prediction of vortex-induced vibration response by employing controlled motion", *Journal of Fluid Mechanics*, Vol.634, pp. 5-39, 2009.

[7] K. Vikestad, J.K. Vandiver, and C.M. Larsen, "Added mass and oscillation frequency for a circular cylinder subjected to vortex-induced vibrations and external disturbance", *Journal of Fluids and Structures*, Vol.14, No.7, pp. 1071-1088, 2000.